Supplement of Atmos. Chem. Phys., 23, 6319–6338, 2023
https://doi.org/10.5194/acp-23-6319-2023-supplement
© Author(s) 2023. CC BY 4.0 License.

Atmospheric Chemistry and Physics
Open Access
EGU

Supplement of

Technical note: Constraining the hydroxyl (OH) radical in the tropics with satellite observations of its drivers – first steps toward assessing the feasibility of a global observation strategy

Daniel C. Anderson et al.

Correspondence to: Daniel C. Anderson (daniel.c.anderson@nasa.gov)

The copyright of individual parts of the supplement might differ from the article licence.

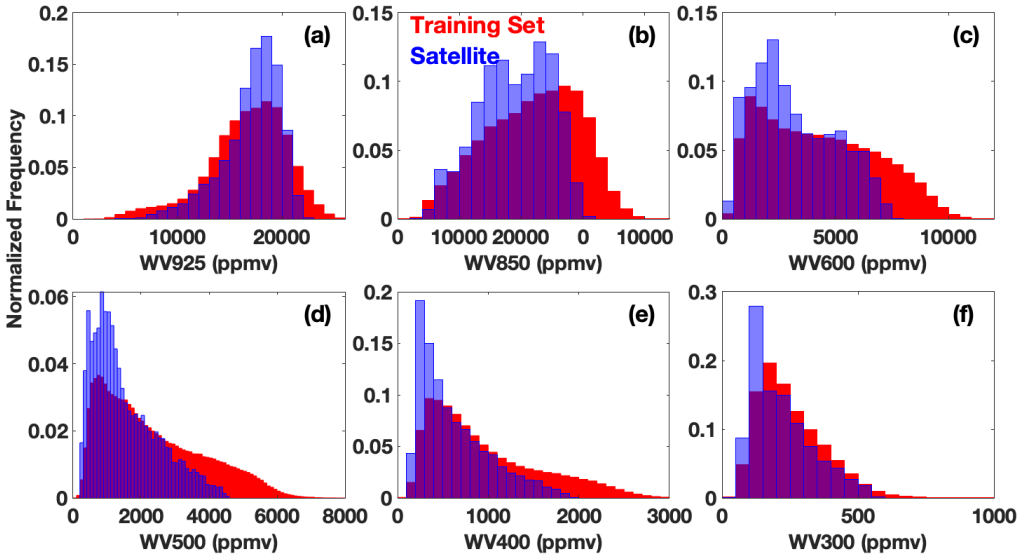

Figure S1: Comparison of the normalized distributions of the training dataset (red) for the February model and satellite observations of the indicated species for February 2017 (blue). Purple indicates regions of overlap.

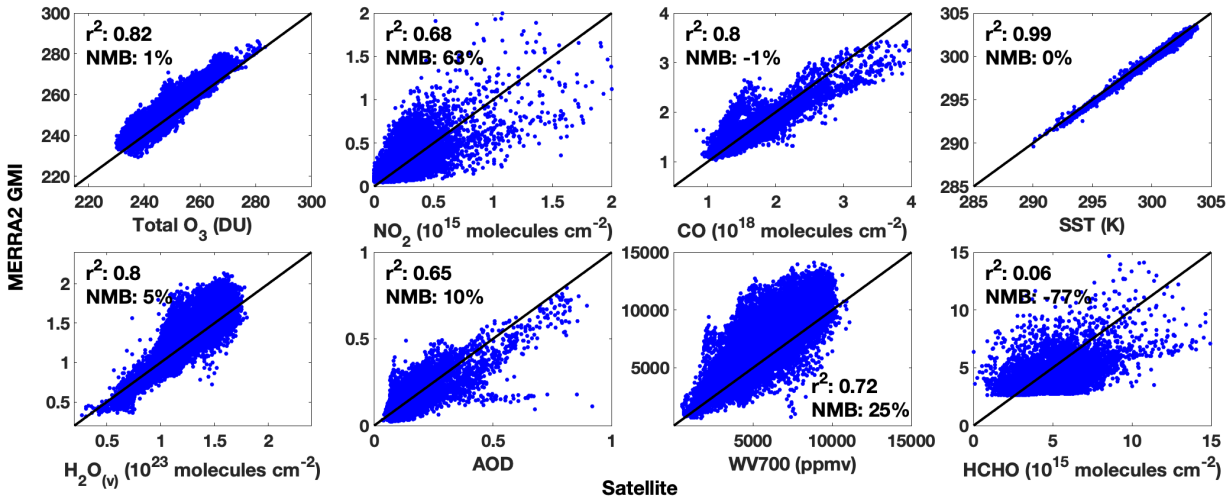

Figure S2: Regression of the indicated species from the MERRA2 GMI simulation against observations from the satellites listed in Table 1 for Feb. 2017. The r^2 of a linear least squares regression as well as the normalized mean bias is also indicated.

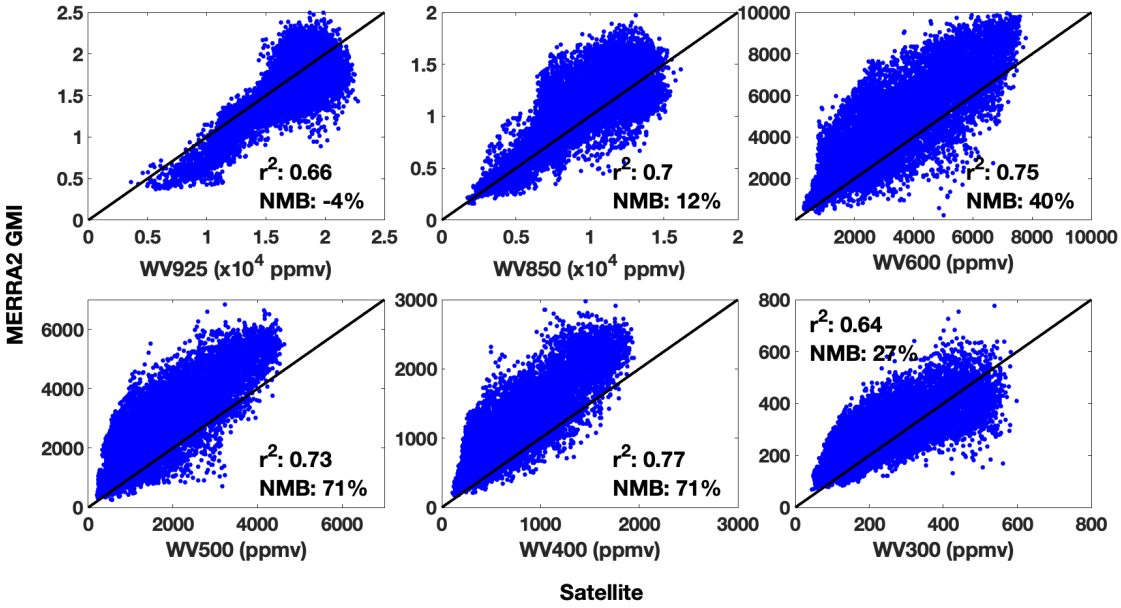

Figure S3: Same as Figure S2 except for the remaining water vapor layers.

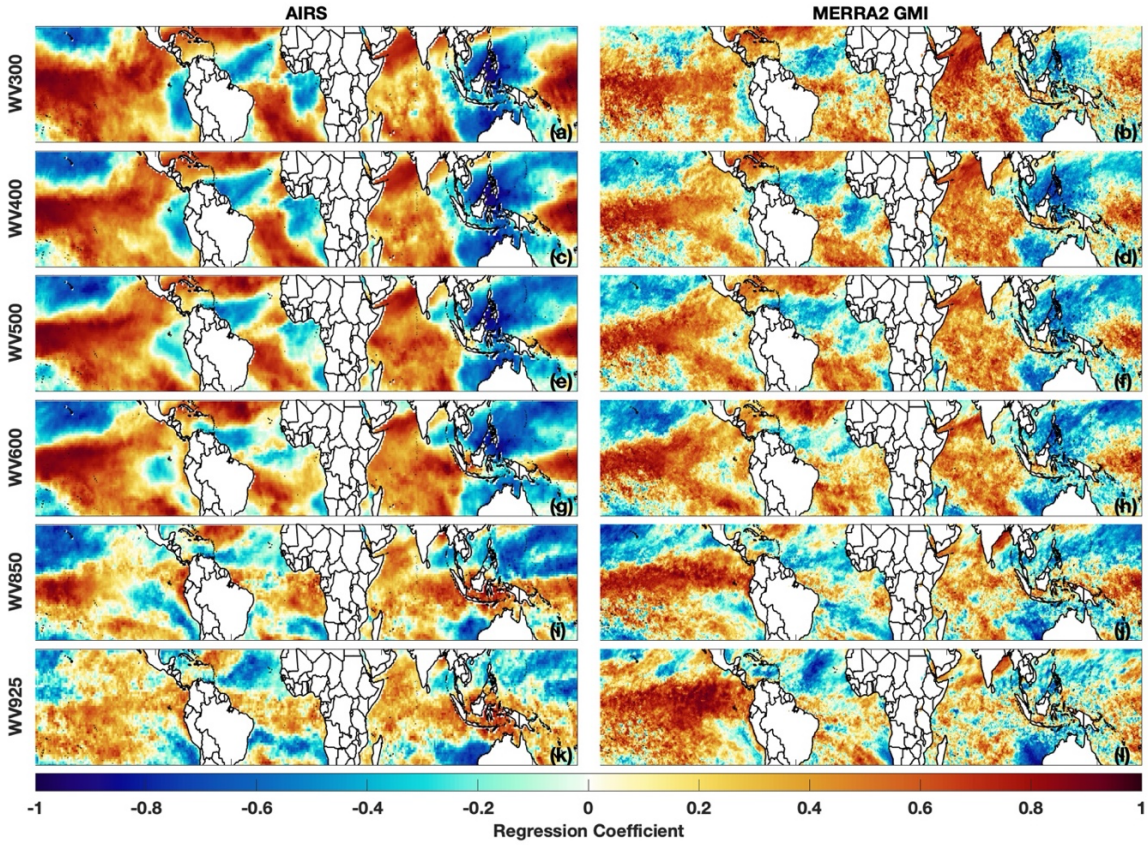

Figure S4: Same as Figure 2 except for the remaining water vapor layers. Regressions are for 2005 – 2019.

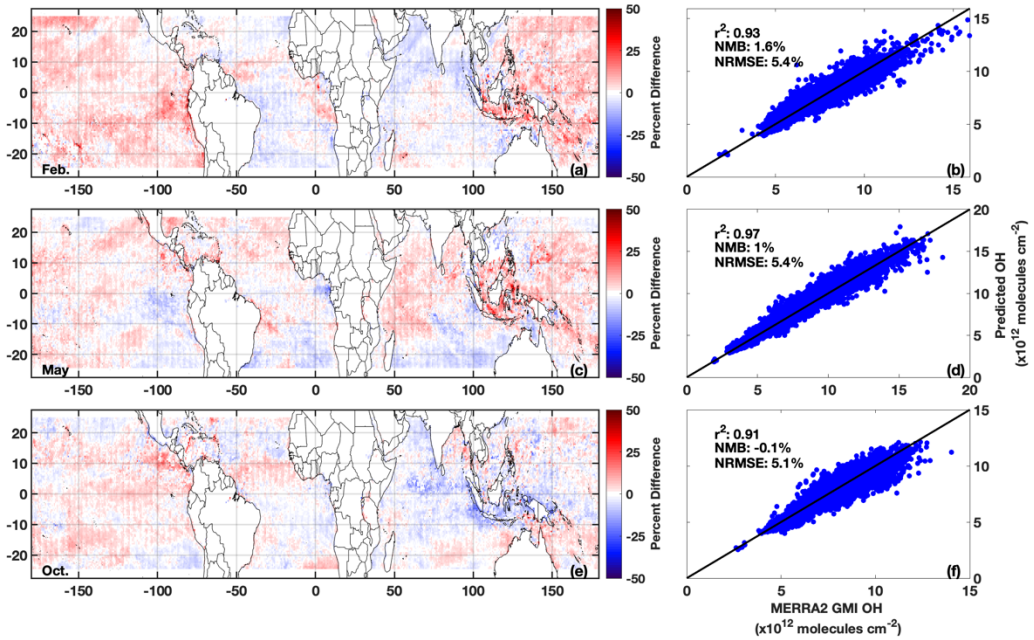

Figure S5: The percent difference between TCOH predicted from the GBRT model and from the MERRA2 GMI simulation for Feb. (a), May (c), and Oct. (e) 2017 is shown on the left. The regression of TCOH from MERRA2 GMI against that predicted from the GBRT model for those months is shown on the right. In addition, the r^2 of a linear least squares fit, the normalized mean bias, and the normalized root mean square error for each month are also indicated.

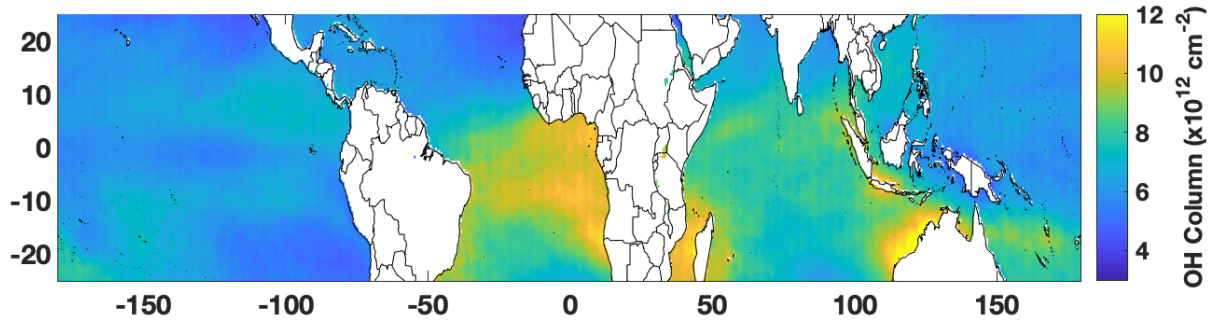

Figure S6: TCOH from MERRA2 GMI for Feb. 2017.

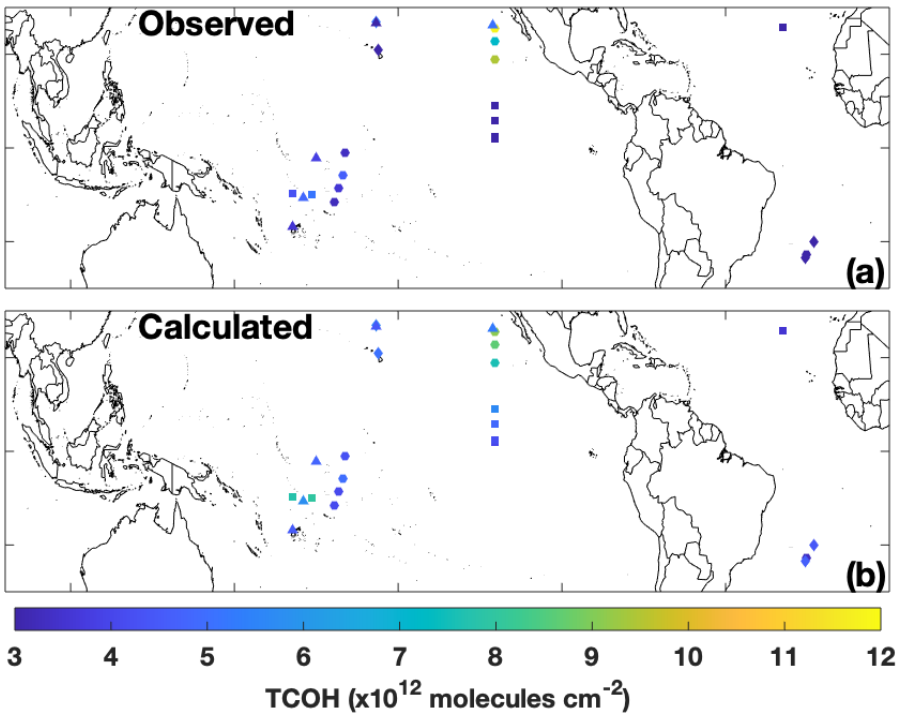

Figure S7: Distribution of observed (a) and GBRT calculated (b) TCOH columns for the four ATom deployments. Only columns with the required GBRT model inputs are shown. Indvidual ATom deployments are shown with circles (ATom 1), squares (ATom 2), diamonds (ATom 3), and triangles (ATom 4).

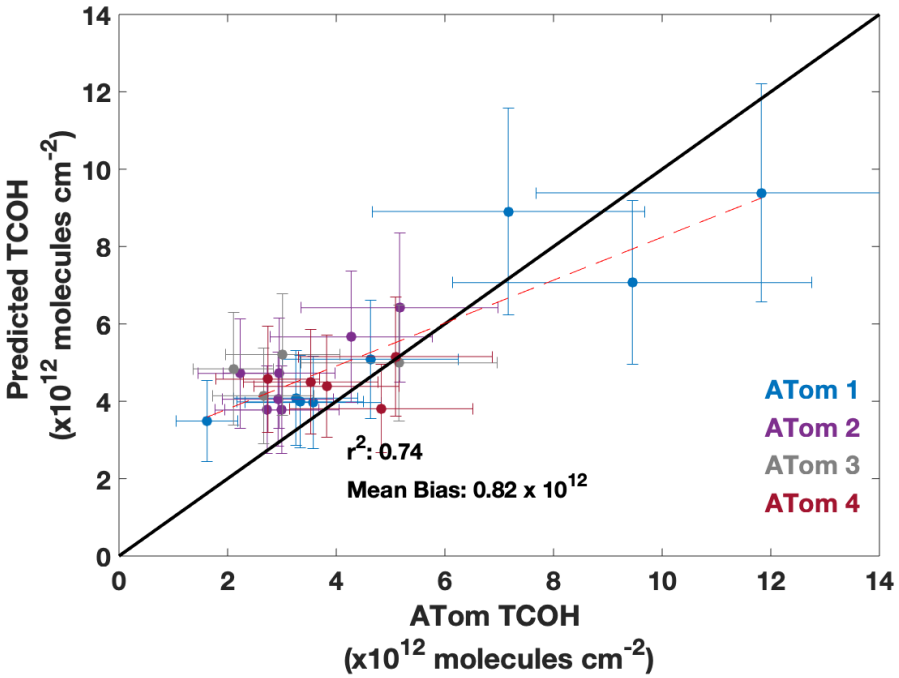

Figure S8: Same as Figure 5 except using a GBRT model that omits NO_2 as an input.

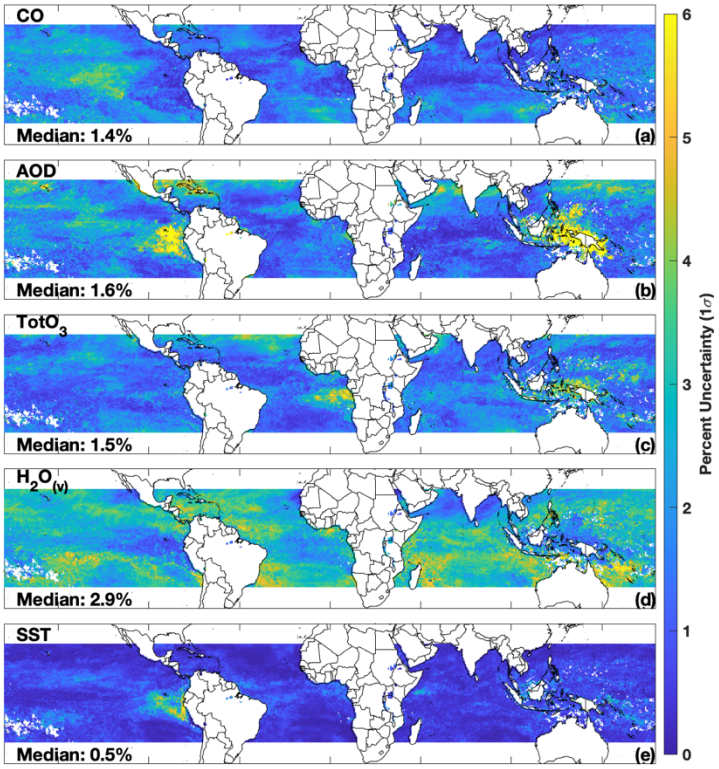

Figure S9: Normalized 1σ uncertainty in the satellite TCOH product due to uncertainties in the indicated retrievals for February 2017.

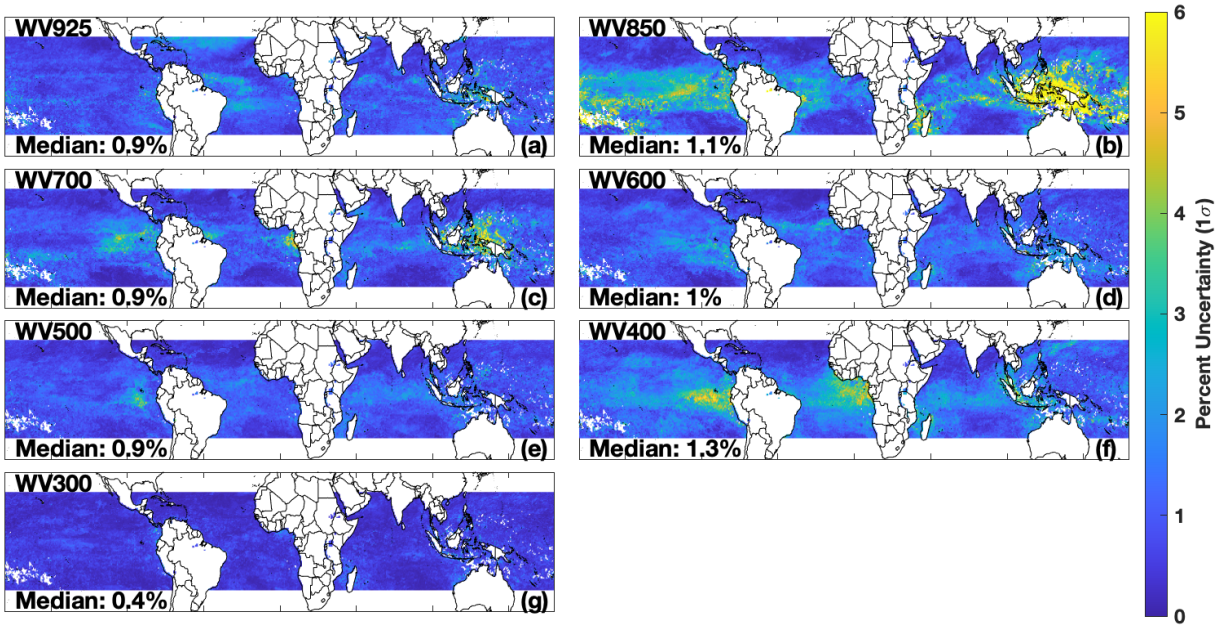

Figure S10: *Same as Figure S9 except for the water vapor layers.*

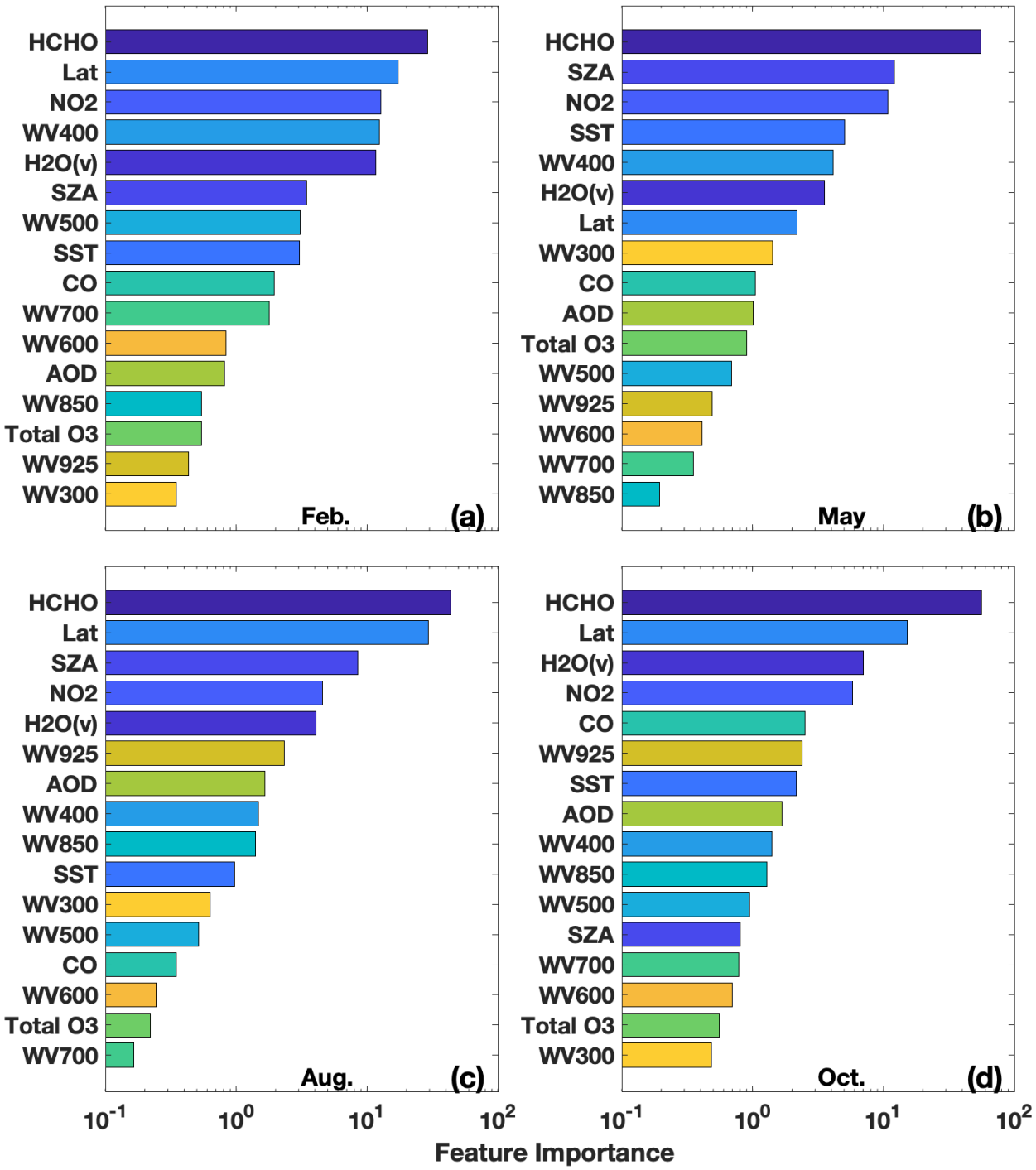

Figure S11: Feature importance, sorted by value, for the GBRT models for February (a), May (b), August (c), and October (d). Bars are colored so that variables have the same color in each panel.

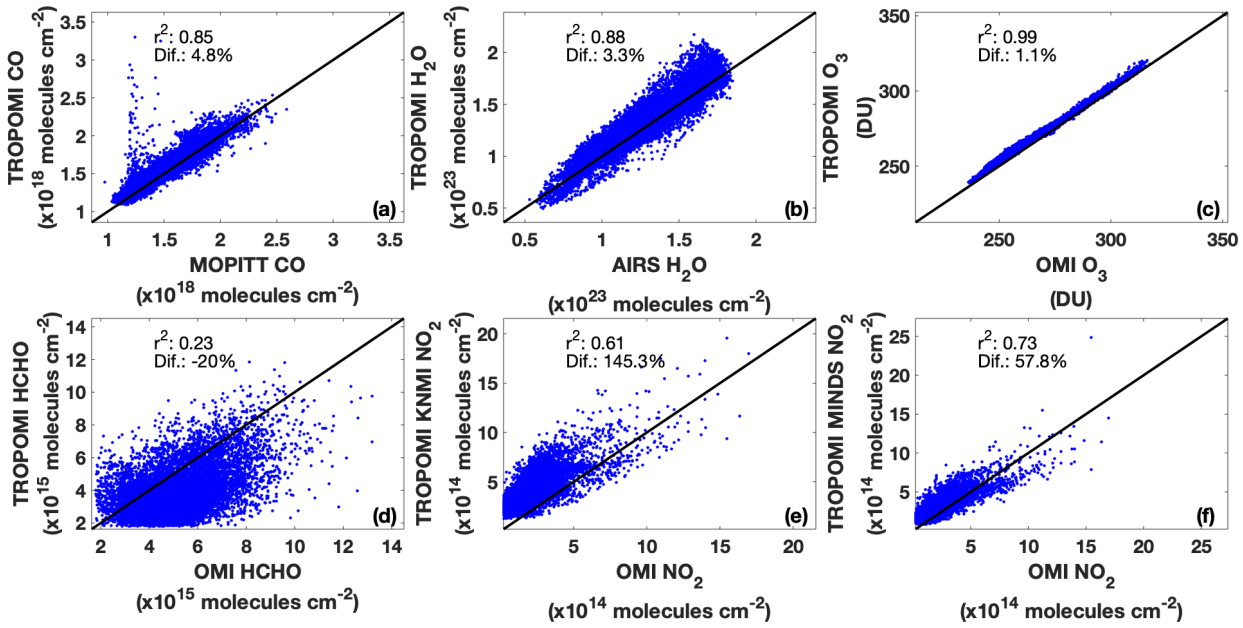

Figure S12: Regression of the indicated species from TROPOMI against retrievals from the satellites listed in Table 1 for May 2018. Both the KNMI (c) and MINDS (f) TROPOMI NO_2 retrievals are shown. We also indicate the r^2 of a linear least squares fit to the data as well as the percent difference between TROPOMI and the other satellite products.

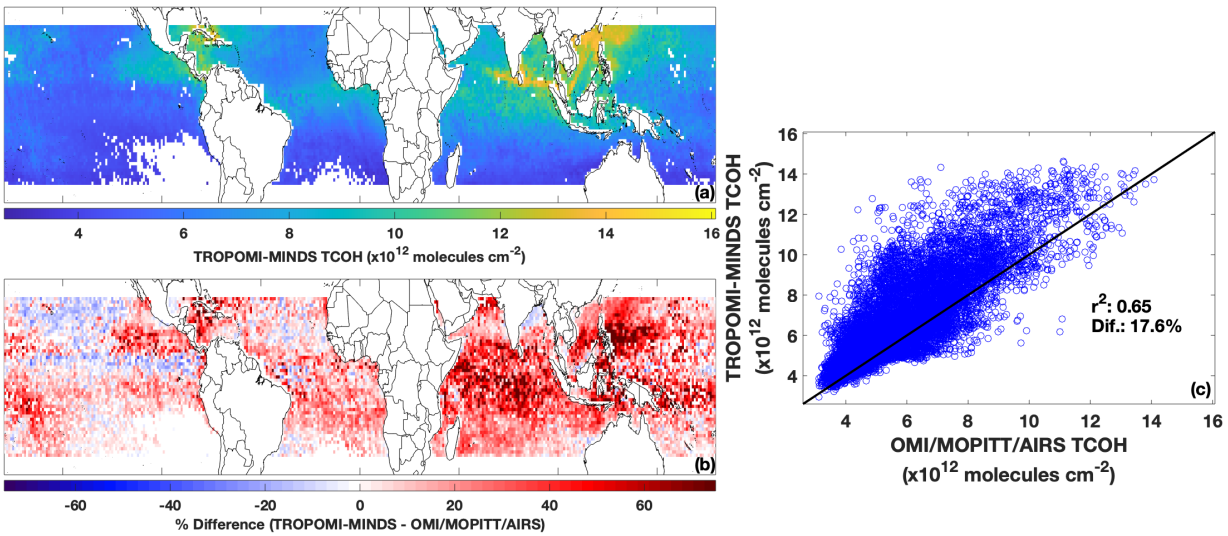

Figure S13: *Same as Figure 7 except using the MINDS NO_2 retrieval for TROPOMI.*

Table S1: Estimated uncertainty and source for each satellite retrieval.

Species	Estimated Uncertainty	Uncertainty Source and Notes
Total O_3 Column	5%	Based on agreement with other observations (Labow et al., 2013)
Tropospheric NO_2 Column	100%	Typical uncertainty of a single retrieval in the remote atmosphere (Choi et al., 2020)
CO Column	5.3%	Median reported uncertainty in L3 data file for study area
HCHO Column	100%	Median reported fit uncertainty of a single retrieval in data file for study area.
$H_2O_{(v)}$ Column	12%	Median reported uncertainty in L3 data file for study area.
SST	0.35 K	Mean bias of dataset when compared to other SST records (Chin et al., 2017)
AOD at 550 nm	$0.05 + 0.15\tau$	Reported value in (Sayer et al., 2014)
$H_2O_{(v)}$ Layers	30 – 40%	Median reported uncertainty in L3 data file for study area.

References

Chin, T. M., Vazquez-Cuervo, J., and Armstrong, E. M.: A multi-scale high-resolution analysis of global sea surface temperature, Remote Sensing of Environment, 200, 154-169, https://doi.org/10.1016/j.rse.2017.07.029, 2017.

Choi, S., Lamsal, L. N., Follette-Cook, M., Joiner, J., Krotkov, N. A., Swartz, W. H., Pickering, K. E., Loughner, C. P., Appel, W., Pfister, G., Saide, P. E., Cohen, R. C., Weinheimer, A. J., and Herman, J. R.: Assessment of NO2 observations during DISCOVER-AQ and KORUS-AQ field campaigns, Atmos. Meas. Tech., 13, 2523-2546, 10.5194/amt-13-2523-2020, 2020.

Labow, G. J., McPeters, R. D., Bhartia, P. K., and Kramarova, N.: A comparison of 40 years of SBUV measurements of column ozone with data from the Dobson/Brewer network, Journal of Geophysical Research: Atmospheres, 118, 7370-7378, https://doi.org/10.1002/jgrd.50503, 2013.

Sayer, A. M., Munchak, L. A., Hsu, N. C., Levy, R. C., Bettenhausen, C., and Jeong, M. J.: MODIS Collection 6 aerosol products: Comparison between Aqua's e-Deep Blue, Dark Target, and "merged" data sets, and usage recommendations, Journal of Geophysical Research: Atmospheres, 119, 13,965-913,989, https://doi.org/10.1002/2014JD022453, 2014.